

# Probing the Majorana mass scale of right-handed neutrinos in mSUGRA

F. Deppisch\*, H. Päs†, A. Redelbach‡, R. Rückl§

*Institut für Theoretische Physik und Astrophysik  
Universität Würzburg  
D-97074 Würzburg, Germany*

Y. Shimizu¶

*Department of Physics  
Nagoya University  
Nagoya, 464-8602, Japan*

## Abstract

We discuss the perspectives of testing the right-handed Majorana mass scale  $M_R$  of the SUSY see-saw model in the mSUGRA framework. Lepton-flavor violating low energy processes are analyzed in recently proposed post-LEP benchmark scenarios, taking into account present uncertainties and future developments in the neutrino sector. Nonobservation of  $\mu \rightarrow e\gamma$  in the next-generation PSI experiment will provide upper bounds on  $M_R$  of the order of  $10^{12\div 14}$  GeV, while on the other hand, a positive signal for  $\tau \rightarrow \mu\gamma$  at SUPERKEKB or the LHC may determine  $M_R$  for a given mSUGRA scenario with an accuracy of a factor of 2.

---

\*E-mail: deppisch@physik.uni-wuerzburg.de

†E-mail: paes@physik.uni-wuerzburg.de

‡E-mail: asredelb@physik.uni-wuerzburg.de

§E-mail: rueckl@physik.uni-wuerzburg.de

¶E-mail: shimizu@eken.phys.nagoya-u.ac.jp

# 1 Introduction

With the evidence for neutrino masses and mixing in solar [1] and atmospheric [2] neutrino experiments, studies of the lepton sector have gained importance as a path to physics beyond the Standard Model. The most elegant and widely accepted explanation for small neutrino masses is provided by the see-saw mechanism [3], in which a large Majorana mass scale  $M_R$  of right-handed neutrinos drives the light neutrino masses down to or below the sub-eV scale, as required by the experimental evidence. A priori, the fundamental scale  $M_R$  can be of the order of the GUT scale, and may thus be inaccessible for any kind of direct experimental tests. However, neutrino mixing implies lepton-flavor violation (LFV), which is absent in the Standard Model and provides indirect probes of  $M_R$ . While lepton-flavor violating processes are suppressed due to the small neutrino masses if only right-handed neutrinos are added to the Standard Model [4], in supersymmetric models new sources of LFV exist. For example, virtual effects of the massive neutrinos affect the renormalization group equations (RGE) of the slepton mass and the trilinear coupling matrices, and give rise to non-diagonal terms inducing LFV.

Assuming the experimentally favored large mixing angle (LMA) MSW solution of the solar neutrino anomaly, one can expect lepton-flavor violating  $\mu$  and  $\tau$  decays with branching ratios close to the current experimental bounds [5]. Some of the existing bounds will be improved significantly in the near future. The current experimental limits (future sensitivities) on low-energy lepton-flavor violating processes involving charged leptons can be summarized as follows:

- $Br(\mu \rightarrow e\gamma) < 1.2 \cdot 10^{-11}(10^{-14})$  [6, 7]
- $Br(\tau \rightarrow e\gamma) < 2.7 \cdot 10^{-6}$  [8]
- $Br(\tau \rightarrow \mu\gamma) < 1.1 \cdot 10^{-6}(10^{-9})$  [9, 10] (1)
- $Br(\mu^+ \rightarrow e^+e^+e^-) < 1.0 \cdot 10^{-12}$  [11]
- $R(\mu^-Ti \rightarrow e^-Ti) < 6.1 \cdot 10^{-13}(10^{-14})$  [12, 13]

Here, the observable  $R$  denotes the cross-section normalized to the total muon capture rate. The MECO experiment aims at a sensitivity for  $\mu^-Al \rightarrow e^-Al$  below  $R \approx 10^{-16}$  [14]. In the farther future, the PRISM project plans to provide beams of low-energy muons with an intensity increased by several orders of magnitude, so that it may become possible to reach  $Br(\mu \rightarrow e\gamma) \approx 10^{-15}$  [15],  $Br(\mu^+ \rightarrow e^+e^+e^-) \approx 10^{-16}$  [16] and  $R(\mu^-Ti \rightarrow e^-Ti) \approx 10^{-18}$  [17] (see also the review [18]). Searches for  $\tau \rightarrow \mu\gamma$  at the LHC or SUPERKEKB are expected to probe LFV in this channel at the level of  $Br \approx 10^{-9}$  [10].

The above processes in the context of supersymmetric see-saw models have been considered in several previous studies (see e.g. [5, 19, 20, 21, 22, 23, 24]). In [19] it has been pointed out that the corresponding branching ratios and cross-sections exhibit a quadratic dependence on the right-handed Majorana neutrino mass scale  $M_R$ . Therefore, the exploration of these processes provides very interesting possibilities to constrain  $M_R$ . In the present paper, we sharpen the current knowledge of these constraints by investigating in more detail which information about the right-handed Majorana masses can be extracted from measurements of the processes (1). It is assumed that the right-handed Majorana masses are degenerate at the scale  $M_R$ . We focus on the recently proposed post-LEP mSUGRA benchmark scenarios [25], and take into account the uncertainties in the neutrino parameters. In addition, we show by how much the sensitivity to  $M_R$  will improve with future more precise neutrino data. Our work updates and extends previous studies in several directions. Firstly, the mSUGRA scenarios of [25] have been developed particularly for linear collider studies, but have not yet been applied to lepton-flavor violating processes at low energies. Our study clarifies the model-dependence of the latter for this very relevant set of mSUGRA models. Secondly, the neutrino input in our analysis is varied in the ranges allowed by present data. The results are compared to expectations for more precise neutrino measurements in the future. Thirdly, we consider degenerate as well as hierarchical neutrino spectra, and study the impact, a future determination of the absolute neutrino mass scale would make. Finally, following [26] it is demonstrated that the influence of the mSUGRA scenarios in the tests of  $M_R$  can be reduced by normalizing  $Br(l_i \rightarrow l_j \gamma)$  to the corresponding SUSY contribution to the muon anomalous magnetic moment.

The paper is organized as follows. In section 2, we discuss the supersymmetric see-saw mechanism and the renormalization group evolution of the neutrino and slepton mass matrices. In section 3, the rare decays  $l_i \rightarrow l_j \gamma$ ,  $\mu \rightarrow 3e$  as well as  $\mu$ - $e$  conversion in nuclei are briefly reviewed, and the most important results for our investigations are displayed. Also the anomalous magnetic moment of the muon and the correlation with  $l_i \rightarrow l_j \gamma$  is discussed there. Section 4 summarizes the input parameters of the mSUGRA benchmark scenarios and the experimental neutrino data used in the analysis. The numerical results of our studies are presented in section 5, and conclusions are drawn in section 6.

## 2 Supersymmetric see-saw mechanism

The supersymmetric see-saw mechanism is described by the term [20]

$$W_\nu = -\frac{1}{2}\nu_R^{cT} M \nu_R^c + \nu_R^{cT} Y_\nu L \cdot H_2 \quad (2)$$

in the superpotential, where  $\nu_{Ra}$  ( $a = e, \mu, \tau$ ) are the right-handed neutrino singlet fields,  $L_a$  denote the left-handed lepton doublets and  $H_2$  is the Higgs doublet with hypercharge  $+\frac{1}{2}$ . The  $3 \times 3$  matrix  $M$  is the Majorana mass matrix, while  $Y_\nu$  is the matrix of neutrino Yukawa couplings leading to the Dirac mass matrix  $m_D = Y_\nu \langle H_2^0 \rangle$ ,  $\langle H_2^0 \rangle = v \sin \beta$  being the  $H_2$  vacuum expectation value with  $v = 174$  GeV and  $\tan \beta = \frac{\langle H_2^0 \rangle}{\langle H_1^0 \rangle}$ . Light neutrinos can be naturally explained if one assumes that the Majorana scale  $M_R$  of the mass matrix  $M$  is much larger than the scale of the Dirac mass matrix  $m_D$ , which is of the order of the electroweak scale. At energies much smaller than  $M_R$  one has an effective superpotential with

$$W_\nu^{eff} = \frac{1}{2}(Y_\nu L \cdot H_2)^T M^{-1} (Y_\nu L \cdot H_2). \quad (3)$$

The corresponding mass term for the left-handed neutrinos  $\nu_{La}$  is then given by

$$-\frac{1}{2}\nu_L^T M_\nu \nu_L + h.c., \quad (4)$$

where the mass matrix

$$M_\nu = m_D^T M^{-1} m_D = Y_\nu^T M^{-1} Y_\nu (v \sin \beta)^2 \quad (5)$$

is suppressed by the large Majorana scale  $M_R$ . In the following we work in the basis where the charged lepton Yukawa coupling matrix  $Y_l$ <sup>1</sup> and the Majorana mass matrix  $M$  of the right-handed neutrinos are diagonal, which is always possible. The matrix  $M_\nu$  is diagonalized by the unitary MNS matrix  $U$ ,

$$U^T M_\nu U = \text{diag}(m_1, m_2, m_3), \quad (6)$$

that relates the neutrino flavor and mass eigenstates:

$$\begin{pmatrix} \nu_e \\ \nu_\mu \\ \nu_\tau \end{pmatrix} = U \begin{pmatrix} \nu_1 \\ \nu_2 \\ \nu_3 \end{pmatrix}. \quad (7)$$

---

<sup>1</sup>Therefore, we do not have to discriminate flavor and mass eigenstates for charged leptons, i.e.  $l_{e,\mu,\tau} = l_{1,2,3} = e, \mu, \tau$

In general,  $U$  can be written in the form

$$U = V \cdot \text{diag}(e^{i\phi_1}, e^{i\phi_2}, 1), \quad (8)$$

where  $\phi_1, \phi_2$  are Majorana phases and  $V$  can be parametrized in the standard CKM form:

$$V = \begin{pmatrix} c_{13}c_{12} & c_{13}s_{12} & s_{13}e^{-i\varphi} \\ -c_{23}s_{12} - s_{23}s_{13}c_{12}e^{i\varphi} & c_{23}c_{12} - s_{23}s_{13}s_{12}e^{i\varphi} & s_{23}c_{13} \\ s_{23}s_{12} - c_{23}s_{13}c_{12}e^{i\varphi} & -s_{23}c_{12} - c_{23}s_{13}s_{12}e^{i\varphi} & c_{23}c_{13} \end{pmatrix}. \quad (9)$$

The experimental data on neutrino oscillations determine or at least constrain the mixing matrix  $V$  and the differences of the squared mass eigenvalues  $m_i$  at a scale not far from the electroweak scale. We will therefore identify these two scales in our analysis. Using the results of recent neutrino fits and making some further necessary assumptions on the neutrino spectrum one can reconstruct  $M_\nu(M_Z)$  from (6).

## 2.1 Renormalization group evolution of the neutrino sector

In order to calculate the lepton-flavor violating contributions to the slepton mass matrix in a top-down approach from the unification scale  $M_X \approx 2 \cdot 10^{16}$  GeV to the electroweak scale, we first need to evolve the neutrino mass matrix  $M_\nu(M_Z)$  to  $M_X$ . Below  $M_R$ , the one-loop RGE in the MSSM is given by [27]

$$\frac{d}{dt}M_\nu = \frac{1}{16\pi^2} \left( \left( -6g_2^2 - \frac{6}{5}g_1^2 + \text{Tr}(6Y_U^\dagger Y_U) \right) M_\nu + \left( (Y_l^\dagger Y_l)M_\nu + M_\nu(Y_l^\dagger Y_l)^T \right) \right) \quad (10)$$

with the U(1) and SU(2) gauge couplings  $g_1$  and  $g_2$ , and the Yukawa coupling matrices  $Y_U$  and  $Y_l$  for the charge  $\frac{2}{3}$ -quarks and charged leptons, respectively. The corresponding evolution equations for  $g_{1,2}$ ,  $Y_U$  and  $Y_l$  can be found in [28]. The RGE is linear in  $M_\nu$  and can thus be solved analytically [27]:

$$M_\nu(t) = I(t) \cdot M_\nu(0) \cdot I(t), \quad t = \ln \left( \frac{\mu}{M_Z} \right). \quad (11)$$

Since the evolution is dominated by the gauge and third generation Yukawa couplings one obtains, to a good approximation:

$$I(t) = I_g I_t \text{diag}(1, 1, I_\tau) \quad (12)$$

with

$$I_g(t) = \exp \left( \frac{1}{16\pi^2} \int_0^t (-3g_2^2 - \frac{3}{5}g_1^2) dt' \right) \quad (13)$$

$$I_t(t) = \exp \left( \frac{1}{16\pi^2} \int_0^t 3|Y_t|^2 dt' \right) \quad (14)$$

$$I_\tau(t) = \exp \left( \frac{1}{16\pi^2} \int_0^t |Y_\tau|^2 dt' \right). \quad (15)$$

To calculate these factors, the MSSM RGEs for the gauge and Yukawa couplings are solved in one-loop approximation, neglecting threshold effects.

In order to proceed with the evolution from  $M_R$  to  $M_X$  we use directly the matrix  $Y_\nu$  of the neutrino Yukawa couplings. From (5) and (6) one finds [20]

$$Y_\nu = \frac{1}{v \sin \beta} \text{diag}(\sqrt{M_1}, \sqrt{M_2}, \sqrt{M_3}) \cdot R \cdot \text{diag}(\sqrt{m_1}, \sqrt{m_2}, \sqrt{m_3}) \cdot U^\dagger, \quad (16)$$

where  $M_i$  are the Majorana masses of the right-handed neutrinos and  $R$  is an unknown orthogonal matrix. As we will see, the lepton-flavor violating terms in the slepton mass matrix depend on  $Y_\nu$  only through the combination  $Y_\nu^\dagger Y_\nu$ . In this work, we assume the right-handed Majorana masses to be degenerate at  $M_R$  ( $M_1 = M_2 = M_3 = M_R$ ) and the matrix  $R$  to be real. Then the product  $Y_\nu^\dagger Y_\nu$  simplifies to

$$Y_\nu^\dagger Y_\nu = \frac{M_R}{v^2 \sin^2 \beta} U \cdot \text{diag}(m_1, m_2, m_3) \cdot U^\dagger, \quad (17)$$

thus being independent of  $R$ . Therefore this class of models is highly predictive and often used for phenomenological studies. In addition, one obtains more conservative upper bounds on  $M_R$  for real  $R$  because a complex matrix  $R$  generically leads to larger values of  $Y_\nu^\dagger Y_\nu$  and thus to larger branching ratios  $Br(l_i \rightarrow l_j \gamma)$  as shown in [20]. Furthermore, since the Majorana phases  $\phi_1$  and  $\phi_2$  defined in (8) also drop out in (17),  $U$  can be replaced by  $V$  in (16). Finally, the neutrino masses  $m_i$  and  $V$  are evaluated from  $M_\nu$  at  $M_R$  using (6). The resulting matrix  $Y_\nu(M_R)$  is then evolved from  $M_R$  to  $M_X$  using the one-loop RGE [20]

$$\frac{d}{dt} Y_\nu = \frac{1}{16\pi^2} Y_\nu \left( \left( -3g_2^2 - \frac{3}{5}g_1^2 + \text{Tr}(3Y_U^\dagger Y_U + Y_\nu^\dagger Y_\nu) \right) \mathbf{1} + Y_l^\dagger Y_l + 3Y_\nu^\dagger Y_\nu \right), \quad (18)$$

and keeping the product  $Y_\nu^\dagger Y_\nu$  on the r.h.s. of (18) fixed at  $M_R$ . The running of the right-handed mass matrix  $M$  between  $M_R$  and  $M_X$  is negligible, as we have checked numerically.

## 2.2 Renormalization group evolution of the slepton sector

Having evolved the neutrino Yukawa couplings or, more specifically, the product  $Y_\nu^\dagger Y_\nu$ , to the unification scale  $M_X$ , one can now run the slepton mass matrix from  $M_X$  to the electroweak scale assuming the mSUGRA universality conditions at  $M_X$ :

$$m_L^2 = m_0^2 \mathbf{1}, \quad m_R^2 = m_0^2 \mathbf{1}, \quad A = A_0 Y_l, \quad (19)$$

where  $m_0$  is the common scalar mass and  $A_0$  is the common trilinear coupling. For the present analysis, we adopt the mSUGRA benchmark scenarios proposed recently in [25] for

linear collider studies. The charged slepton (mass)<sup>2</sup> matrix has the form:

$$m_{\tilde{l}}^2 = \begin{pmatrix} m_{\tilde{l}_L}^2 & (m_{\tilde{l}_{LR}}^2)^\dagger \\ m_{\tilde{l}_{LR}}^2 & m_{\tilde{l}_R}^2 \end{pmatrix}, \quad (20)$$

where  $m_{\tilde{l}_L}^2$ ,  $m_{\tilde{l}_R}^2$  and  $m_{\tilde{l}_{LR}}^2$  are  $3 \times 3$  matrices,  $m_{\tilde{l}_L}^2$  and  $m_{\tilde{l}_R}^2$  being hermitian. The matrix elements are given by

$$(m_{\tilde{l}_L}^2)_{ab} = (m_L^2)_{ab} + \delta_{ab} \left( m_{l_a}^2 + m_Z^2 \cos(2\beta) \left( -\frac{1}{2} + \sin^2 \theta_W \right) \right) \quad (21)$$

$$(m_{\tilde{l}_R}^2)_{ab} = (m_R^2)_{ab} + \delta_{ab} (m_{l_a}^2 - m_Z^2 \cos(2\beta) \sin^2 \theta_W) \quad (22)$$

$$(m_{\tilde{l}_{LR}}^2)_{ab} = A_{ab} v \cos \beta - \delta_{ab} m_{l_a} \mu \tan \beta, \quad (23)$$

$\theta_W$  being the Weinberg angle and  $\mu$  the SUSY Higgs-mixing parameter. After evolution from  $M_X$  to  $M_Z$ , one has

$$m_L^2 = m_0^2 \mathbf{1} + (\delta m_L^2)_{\text{MSSM}} + \delta m_L^2 \quad (24)$$

$$m_R^2 = m_0^2 \mathbf{1} + (\delta m_R^2)_{\text{MSSM}} + \delta m_R^2 \quad (25)$$

$$A = A_0 Y_l + \delta A_{\text{MSSM}} + \delta A, \quad (26)$$

where  $(\delta m_{L,R}^2)_{\text{MSSM}}$  and  $(\delta A)_{\text{MSSM}}$  denote the usual MSSM renormalization-group corrections [28] which are flavor-diagonal. In addition, the presence of right-handed neutrinos radiatively induces flavor off-diagonal terms denoted by  $\delta m_{L,R}^2$  and  $\delta A$  in (24) to (26). These corrections are taken into account in the approximation [19]

$$\delta m_L^2 = -\frac{1}{8\pi^2} (3m_0^2 + A_0^2) (Y_\nu^\dagger Y_\nu) \ln \left( \frac{M_X}{M_R} \right) \quad (27)$$

$$\delta m_R^2 = 0 \quad (28)$$

$$\delta A = -\frac{3A_0}{16\pi^2} (Y_l Y_\nu^\dagger Y_\nu) \ln \left( \frac{M_X}{M_R} \right). \quad (29)$$

It is these terms which give rise to lepton-flavor violating processes such as  $l_i \rightarrow l_j \gamma$  and  $\mu$ -e conversion.

The physical charged slepton masses are then found by diagonalizing (20) using the  $6 \times 6$  unitary matrix  $U_{\tilde{l}}$ :

$$U_{\tilde{l}}^\dagger m_{\tilde{l}}^2 U_{\tilde{l}} = \text{diag}(m_{\tilde{l}_1}^2, \dots, m_{\tilde{l}_i}^2, \dots, m_{\tilde{l}_6}^2). \quad (30)$$

Correspondingly, the slepton mass eigenstates are expressed in terms of the gauge eigenstates by

$$\tilde{l}_i = (U_{\tilde{l}}^*)_{ai} \tilde{l}_{La} + (U_{\tilde{l}}^*)_{(a+3)i} \tilde{l}_{Ra}, \quad i = 1, \dots, 6; \quad a = e, \mu, \tau. \quad (31)$$

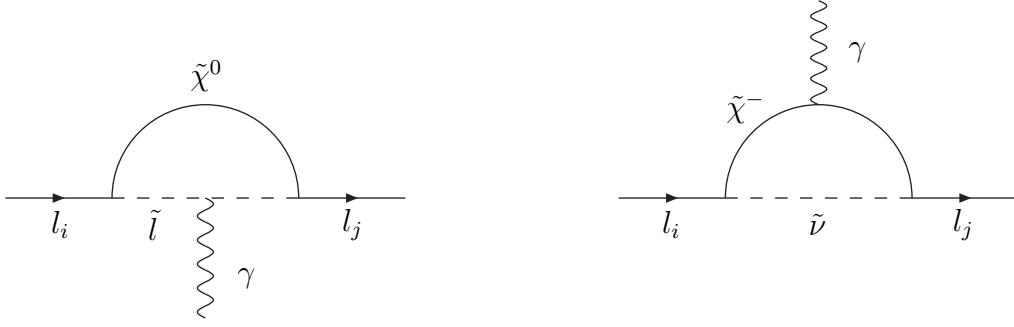


Figure 1: Diagrams for  $l_i^- \rightarrow l_j^- \gamma$  in the MSSM

Similarly to (21), the  $3 \times 3$  (mass)<sup>2</sup> matrix of the SUSY partners of the left-handed neutrinos is given by

$$(m_{\tilde{\nu}}^2)_{ab} = (m_L^2)_{ab} + \frac{1}{2} \delta_{ab} m_Z^2 \cos(2\beta), \quad (32)$$

where  $m_L^2$  can be taken from (24). The partners of the right-handed neutrinos are very heavy and can therefore be disregarded. After diagonalization with the unitary  $3 \times 3$  matrix  $U_{\tilde{\nu}}$ ,

$$U_{\tilde{\nu}}^\dagger m_{\tilde{\nu}}^2 U_{\tilde{\nu}} = \text{diag}(m_{\tilde{\nu}_1}^2, m_{\tilde{\nu}_2}^2, m_{\tilde{\nu}_3}^2), \quad (33)$$

the mass eigenstates  $\tilde{\nu}_i$  are related to the gauge eigenstates by

$$\begin{pmatrix} \tilde{\nu}_e \\ \tilde{\nu}_\mu \\ \tilde{\nu}_\tau \end{pmatrix} = U_{\tilde{\nu}} \begin{pmatrix} \tilde{\nu}_1 \\ \tilde{\nu}_2 \\ \tilde{\nu}_3 \end{pmatrix}. \quad (34)$$

### 3 LFV low-energy processes and $g_\mu - 2$

#### 3.1 The radiative decays $l_i \rightarrow l_j \gamma$

The effective Lagrangian for  $l_i^- \rightarrow l_j^- \gamma$  is given by [26]

$$\mathcal{L}_{eff} = \frac{e}{2} \bar{l}_j \sigma_{\alpha\beta} F^{\alpha\beta} \left( A_L^{ij} P_L + A_R^{ij} P_R \right) l_i, \quad (35)$$

where  $F^{\alpha\beta}$  is the electromagnetic field strength tensor,  $\sigma_{\alpha\beta} = \frac{i}{2} [\gamma_\alpha, \gamma_\beta]$  and  $P_{R,L} = \frac{1}{2}(1 \pm \gamma_5)$  are the helicity projection operators. The coefficients  $A_{L,R}^{ij}$  are determined by the photon penguin diagrams shown in Fig. 1 with charginos/sneutrinos or neutralinos/charged sleptons in the loop.



From (35) one obtains the following decay rate for  $l_i^- \rightarrow l_j^- \gamma$  [5]:

$$\Gamma(l_i^- \rightarrow l_j^- \gamma) = \frac{\alpha}{4} m_{l_i}^3 \left( |A_L^c + A_L^n|^2 + |A_R^c + A_R^n|^2 \right). \quad (36)$$

The superscript  $c(n)$  refers to the chargino (neutralino) diagram of Fig. 1, while the flavor indices are omitted. Because  $m_{l_i} \gg m_{l_j}$  and  $m_{\tilde{l}_R}^2$  is diagonal (see (22), (25) and (28)), one has  $A_R \gg A_L$  [19], [20]. The dominant amplitudes in (36) are approximately given by

$$\begin{aligned} A_R^c &\simeq \frac{1}{32\pi^2} \frac{g_2^2 m_{l_i}}{\sqrt{2} m_W \cos \beta} \sum_{a=1}^2 \sum_{k=1}^3 \frac{m_{\tilde{\chi}_a^-}}{m_{\tilde{\nu}_k}^2} (O_R)_{a1} (O_L)_{a2} (U_{\tilde{\nu}}^*)_{jk} (U_{\tilde{\nu}})_{ik} \\ &\times \frac{1}{(1 - r_{ak}^c)^3} \left( -3 + 4r_{ak}^c - (r_{ak}^c)^2 - 2 \ln r_{ak}^c \right) \end{aligned} \quad (37)$$

$$\begin{aligned} A_R^n &\simeq -\frac{1}{32\pi^2} g_2^2 \tan \theta_W \sum_{a=1}^4 \sum_{k=1}^6 \frac{m_{\tilde{\chi}_a^0}}{m_{\tilde{l}_k}^2} (O_N)_{a1} ((O_N)_{a2} + (O_N)_{a1} \tan \theta_W) \\ &\times (U_{\tilde{l}}^*)_{jk} (U_{\tilde{l}})_{(i+3)k} \frac{1}{(1 - r_{ak}^n)^3} \left( 1 - (r_{ak}^n)^2 + 2r_{ak}^n \ln r_{ak}^n \right) \end{aligned} \quad (38)$$

with

$$r_{ak}^c = \left( \frac{m_{\tilde{\chi}_a^-}}{m_{\tilde{\nu}_k}} \right)^2, \quad r_{ak}^n = \left( \frac{m_{\tilde{\chi}_a^0}}{m_{\tilde{l}_k}} \right)^2, \quad (39)$$

the chargino diagonalization matrices  $O_L$ ,  $O_R$  and the neutralino diagonalization matrix  $O_N$ . The mass eigenvalues of the charginos and neutralinos are denoted by  $m_{\tilde{\chi}_a^-}$  and  $m_{\tilde{\chi}_a^0}$ , respectively. The numerical calculations discussed later are performed with the full expressions for  $A_L^{c,n}$  and  $A_R^{c,n}$ , which can be found in [5] and [30].

Note that there is no difference between the rates of  $l_i^- \rightarrow l_j^- \gamma$  and  $l_i^+ \rightarrow l_j^+ \gamma$  at the one-loop level and no CP violating observables can be constructed at this level of perturbation theory [30, 31]. We therefore do not distinguish between  $Br(l_i^- \rightarrow l_j^- \gamma)$  and  $Br(l_i^+ \rightarrow l_j^+ \gamma)$  in the following.

### 3.2 $Br(\mu \rightarrow 3e)$ and $R(\mu^- N \rightarrow e^- N)$

The processes  $\mu \rightarrow 3e$  and  $\mu^- N \rightarrow e^- N$  are dominated by photon penguin contributions. As a consequence, one has the following model-independent relations [19]:

$$\frac{Br(\mu \rightarrow 3e)}{Br(\mu \rightarrow e\gamma)} \approx \frac{\alpha}{8\pi} \frac{8}{3} \left( \ln \frac{m_\mu^2}{m_e^2} - \frac{11}{4} \right) \approx 7 \cdot 10^{-3} \quad (40)$$

$$\frac{R(\mu^- N \rightarrow e^- N)}{Br(\mu \rightarrow e\gamma)} \approx \frac{\Gamma_\mu}{\Gamma_{cap}} 16\alpha^4 Z_{eff}^4 |F(q^2)|^2 \quad (41)$$

$$\approx 6 \cdot 10^{-3} \quad \text{for Titanium,} \quad (42)$$

where  $\Gamma_\mu$  is the total decay width of the muon,  $F(q^2)$  is the nuclear form factor and  $Z$  ( $Z_{eff}$ ) is the electric (effective) charge of the nucleus. From the above and (1) one can see that the present experimental upper limits on  $Br(\mu \rightarrow 3e)$  and  $R(\mu^- N \rightarrow e^- N)$  constrain LFV considerably less than the current limit on  $Br(\mu \rightarrow e\gamma)$ . However, a future measurement of  $R$  in the range of  $R(\mu^- Ti \rightarrow e^- Ti) \approx 10^{-18}$  [17] as mentioned in the introduction would provide a more sensitive test than the corresponding future sensitivity  $Br(\mu \rightarrow e\gamma) \approx 10^{-15}$ . We have examined the relations (40) to (42) numerically for the neutrino parameters and mSUGRA scenarios presented in the next section using complete analytic expressions [5], and have found

$$\frac{Br(\mu \rightarrow 3e)}{Br(\mu \rightarrow e\gamma)} \approx (6 - 7) \cdot 10^{-3} \quad (43)$$

$$\frac{R(\mu^- Ti \rightarrow e^- Ti)}{Br(\mu \rightarrow e\gamma)} \approx (5 - 7) \cdot 10^{-3} \quad (44)$$

in good agreement with the above estimates.

### 3.3 Anomalous magnetic moment of the muon

The supersymmetric contribution to  $\frac{1}{2}(g_\mu - 2)$  is described by the diagrams of Fig. 1 for  $i = j = 2$ . In this case the effective Lagrangian (35) yields [26]

$$\delta a_\mu = \frac{m_\mu}{2} (A_R^{22} + A_L^{22}) \quad (45)$$

and, with (36), the relation [26]

$$\frac{Br(l_i \rightarrow l_j \gamma)}{|\delta a_\mu|^2} \simeq \frac{\alpha m_{l_i}^3}{\Gamma_i m_\mu^2} \left| \frac{A_R^{ij}}{A_L^{22} + A_R^{22}} \right|^2, \quad (46)$$

where  $\Gamma_i$  denotes the total decay width of lepton  $l_i$  and  $A_R^{ij} \gg A_L^{ij}$  has been used. It will be shown later that this ratio varies less with the SUSY parameters and thus provides a less model-dependent test of LFV than  $Br(l_i \rightarrow l_j \gamma)$  alone.

## 4 Input parameters

### 4.1 mSUGRA benchmark scenarios

In this paper we focus on the mSUGRA benchmark scenarios proposed in [25]. The theoretical framework of these scenarios is the constrained MSSM with universal soft supersymmetry breaking masses and  $R$ -parity conservation. Sparticle spectra corresponding to these

scenarios are consistent with all experimental and cosmological constraints, in particular with

- direct sparticle searches
- $b \rightarrow s\gamma$
- cosmological relic density, with the lightest neutralino as lightest SUSY particle and dark matter candidate
- Higgs searches

This class of models involves five free parameters: the universal gaugino mass  $m_{1/2}$  and the universal scalar mass  $m_0$  at the GUT scale, the ratio  $\tan\beta$  of the Higgs vacuum expectation values, the sign of the Higgs mixing parameter  $\mu$ , and the universal trilinear coupling parameter  $A_0$ . The values of these parameters for the benchmark scenarios are listed in Tab. 1.  $A_0$  is set to zero in all scenarios. Further details can be found in [25].

Scenario	$m_{1/2}/\text{GeV}$	$m_0/\text{GeV}$	$\tan\beta$	$\text{sgn}(\mu)$	$\delta a_\mu/10^{-10}$
A	600	140	5	+	2.8
B	250	100	10	+	28
C	400	90	10	+	13
D	525	125	10	-	-7.4
E	300	1500	10	+	1.7
F	1000	3450	10	+	0.29
G	375	120	20	+	27
H	1500	419	20	+	1.7
I	350	180	35	+	45
J	750	300	35	+	11
K	1150	1000	35	-	-3.3
L	450	350	50	+	31
M	1900	1500	50	+	2.1

Table 1: Input parameters of the mSUGRA benchmark scenarios and the predicted shift  $\delta a_\mu$  in  $\frac{1}{2}(g_\mu - 2)$  [25].

Also given in Tab. 1 is the corresponding shift in the muon anomalous magnetic moment. The current  $1.6\sigma$  discrepancy between the measurement of  $\frac{1}{2}(g_\mu - 2)$  and the Standard

Model prediction [32] amounts to

$$\delta a_\mu = (25 \pm 16) \cdot 10^{-10}. \quad (47)$$

Scenarios with relatively light sparticle masses below 500 GeV (e.g. B, C, G, L) are in better agreement with the above value of  $\delta a_\mu$  than scenarios with heavier sparticles (e.g. E, F, H, M). Moreover, (47) favors a positive sign for  $\mu$ .

## 4.2 Neutrino data

Solar and atmospheric neutrino experiments provide clear evidence for neutrino oscillations. The favored interpretation of the experimental results on solar neutrinos suggests  $\nu_e \rightarrow \nu_{\mu,\tau}$  oscillations driven by the mass squared difference  $\Delta m_{12}^2 = m_2^2 - m_1^2$  in the range of the LMA solution, while the results on atmospheric neutrinos are interpreted by  $\nu_\mu \rightarrow \nu_\tau$  oscillations driven by  $\Delta m_{23}^2 = m_3^2 - m_2^2$  in the case of three active neutrinos. For the present analysis, we use the global fits in a three-neutrino framework performed in [33]. In [34] it has been pointed out that the inclusion of the SNO result in a two-neutrino analysis of the solar neutrinos implies only minor changes.

We also consider the improvement in our knowledge of the neutrino sector expected from future neutrino experiments, and discuss the consequences of these future accomplishments for the tests of the Majorana scale  $M_R$  considered in this paper. We always assume the present best fit values of the neutrino parameters to remain unchanged. The future improvements in the experimental errors of these parameters anticipated for a perspective view are summarized below together with other relevant expectations:

- $\Delta m_{12}^2$  and  $\sin^2 2\theta_{12}$ : The long-baseline reactor experiment KAMLAND is designed to test the LMA MSW solution of the solar neutrino problem. Data taking is expected to start in 2002 and the solar neutrino parameters will be determined with an accuracy of  $\delta(\Delta m_{12}^2)/\Delta m_{12}^2 = 10\%$  and  $\delta(\sin^2 2\theta_{12}) = \pm 0.1$  within three years of measurement [35].
- $\Delta m_{23}^2$  and  $\sin^2 2\theta_{23}$ : The atmospheric oscillation parameters will be determined by the long-baseline accelerator experiment MINOS with an accuracy of  $\delta(\Delta m_{23}^2)/\Delta m_{23}^2 = 30\%$  and  $\delta(\sin^2 2\theta_{23}) = \pm 0.1$  [36].
- $\sin^2 2\theta_{13}$ : The CHOOZ reactor experiment restricts the angle  $\theta_{13}$  to  $\sin^2 2\theta_{13} < 0.1$  [37]. The long baseline experiment MINOS [36] can probe the range  $\sin^2 2\theta_{13} \gtrsim 0.02-0.05$ . A future superbeam, a neutrino factory [38] or the analysis of the neutrino

energy spectra of a future galactic supernova [39] may provide a sensitivity at the level of a few times  $10^{-3}$  to  $10^{-4}$ . To explore the potential of future neutrino studies we take  $\delta(\sin^2 2\theta_{13}) = 3 \cdot 10^{-3}$ .

- *The neutrino mass spectra:* The inverse hierarchical spectrum with two heavy and a single light state is disfavored according to a recent analysis [40] of the neutrino spectrum from supernova SN1987A, unless the mixing angle  $\theta_{13}$  is large (compare, however, [41]). We therefore restrict our analysis to the direct (normal) hierarchy. LFV rates for inverse hierarchical schemes lie in the intermediate range between the extreme cases we discuss,  $Br(\text{degenerate}) \ll Br(\text{inverse}) < Br(\text{hierarchy})$ , as pointed out in [24].
- *The Dirac CP phase  $\varphi$ :* Even at a neutrino factory, one will only be able to distinguish  $\varphi = 0$  from  $\pi/2$  if  $\Delta m_{12}^2 > 10^{-5} \text{ eV}^2$ . For this reason we vary  $\varphi$  in the full range  $0 < \varphi < 2\pi$  [42].
- *The neutrino mass scale:* While neutrino oscillation experiments provide information on the neutrino mass squared differences  $\Delta m_{ij}^2$ , the absolute scale of the neutrino masses is not known so far. Upper bounds can be obtained from the neutrino hot dark matter contribution to the cosmological large scale structure evolution and the Cosmic Microwave Background, from the interpretation of the extreme energy cosmic rays in the Z-burst model, tritium beta decay experiments and neutrinoless double beta decay experiments [43]. A next generation double beta decay experiment like GENIUSI, MAJORANA, EXO, XMASS or MOON will test the quantity  $m_{ee} = |\sum_i V_{1i}^2 e^{i2\phi_i} m_i|$  down to  $10^{-2} \text{ eV}$ . Since  $V_{13}^2 = \sin^2 2\theta_{13}/4 < 0.025$ , the contribution of  $m_3$  drops out and a bound  $m_{ee} < 10^{-2} \text{ eV}$  will imply  $m_1 < 10^{-2} \text{ eV} / \cos 2\theta_{12}$ . If one further assumes that KAMLAND measures  $\sin^2 2\theta_{12}$  with  $\delta(\sin^2 2\theta_{12}) = \pm 0.1$ , one obtains the bound  $m_1 < 3 \cdot 10^{-2} \text{ eV}$ . On the other hand, a large mass  $m_1$  could be tested by future tritium beta decay projects. A positive signal at the final sensitivity of the KATRIN experiment would imply  $m_1 = 0.3 \pm 0.1 \text{ eV}$  [44]. Such a value would be compatible with the recent evidence claim for neutrinoless double beta decay [45].

For the present purposes, typical hierarchical and degenerate neutrino mass spectra are parametrized as follows:

(a) hierarchical  $\nu_L$  and degenerate  $\nu_R$ :

$$m_1 \approx 0, \quad m_2 \approx \sqrt{\Delta m_{12}^2}, \quad m_3 \approx \sqrt{\Delta m_{23}^2} \quad (48)$$

$$M_1 = M_2 = M_3 = M_R \quad (49)$$

(b) quasi-degenerate  $\nu_L$  and degenerate  $\nu_R$  [24]:

$$m_1, \quad m_2 \approx m_1 + \frac{1}{2m_1} \Delta m_{12}^2, \quad m_3 \approx m_1 + \frac{1}{2m_1} \Delta m_{23}^2 \quad (50)$$

$$M_1 = M_2 = M_3 = M_R \quad (51)$$

where  $m_1 \gg \sqrt{\Delta m_{23}^2} \gg \sqrt{\Delta m_{12}^2}$ .

The product of Yukawa couplings  $Y_\nu^\dagger Y_\nu$ , appearing in the renormalization group corrections to the left-handed slepton mass matrix (27) can then be approximated by

$$(a) \quad (Y_\nu^\dagger Y_\nu)_{ab} \approx \frac{M_R}{v^2 \sin^2 \beta} \sqrt{\Delta m_{23}^2} \left( \sqrt{\frac{\Delta m_{12}^2}{\Delta m_{23}^2}} V_{a2} V_{b2}^* + V_{a3} V_{b3}^* \right) \quad (52)$$

$$(b) \quad (Y_\nu^\dagger Y_\nu)_{ab} \approx \frac{M_R}{v^2 \sin^2 \beta} \left( m_1 \delta_{ab} + \frac{\Delta m_{23}^2}{2m_1} \left( \frac{\Delta m_{12}^2}{\Delta m_{23}^2} V_{a2} V_{b2}^* + V_{a3} V_{b3}^* \right) \right). \quad (53)$$

In both cases the largest branching ratio for  $l_i \rightarrow l_j \gamma$  is expected in the channel  $\tau \rightarrow \mu \gamma$  because of  $|V_{33} V_{23}^*| \approx |V_{32} V_{22}^*|$  and  $\Delta m_{23}^2 \gg \Delta m_{12}^2$ . The decays  $\mu \rightarrow e \gamma$  and  $\tau \rightarrow e \gamma$  are suppressed by the smallness of  $\Delta m_{12}^2$  and  $V_{13}$ . In the case (b), there is an additional suppression by  $\sqrt{\Delta m_{23}^2}/m_1$  or  $\sqrt{\Delta m_{12}^2}/m_1$  relative to the case (a).

In the following analysis, the neutrino parameters are varied in the ranges specified in Tab. 2, characterizing the present knowledge and future prospects.

parameter	best fit value	present	future
$\tan^2 \theta_{23}$	1.40	+1.64 -1.01	+1.37 -0.66
$\tan^2 \theta_{13}$	0.005	+0.050 -0.005	+0.001 -0.005
$\tan^2 \theta_{12}$	0.36	+0.65 -0.16	+0.35 -0.16
$\Delta m_{12}^2/10^{-5} \text{ eV}^2$	3.30	+66.7 -2.3	+0.3 -0.3
$\Delta m_{23}^2/10^{-3} \text{ eV}^2$	3.10	+3.0 -1.7	+1.0 -1.0
$\varphi/\text{rad}$	0 to $2\pi$		
$m_1/\text{eV}$	0 to 0.03 ( $0.3_{-0.16}^{+0.11}$ )		

Table 2: 90% CL fits of neutrino parameters characterizing the present and future uncertainties. The range of the neutrino mass scale  $m_1$  refers to a hierarchical (degenerate) spectrum.

Note that all parameters are varied simultaneously. The Majorana mass scale  $M_R$  is treated as a free parameter. This contrasts with other approaches [19, 20] where Yukawa coupling unification

$$|Y_{\nu_3}| = Y_t \text{ at } M_X \quad (54)$$

is assumed,  $|Y_{\nu_3}|^2$  being the largest eigenvalue of  $Y_\nu^\dagger Y_\nu$ . Fig. 2 shows the normalized Yukawa coupling  $|Y_{\nu_3}|/Y_t$  at  $M_X$  as a function of the Majorana mass  $M_R$ . One can see that the assumption (54) would fix the Majorana mass scale to  $M_R \approx 4 \cdot 10^{14}$  GeV for hierarchical neutrinos and to  $M_R \approx 7 \cdot 10^{13}$  GeV in the degenerate case.

Fig. 2 also shows that for large values of  $M_R$ , the Yukawa coupling  $|Y_{\nu_3}|$  eventually gets too strong for perturbation theory to be valid. Therefore, we restrict  $|Y_{\nu_3}|$  to values  $\frac{|Y_{\nu_3}|^2}{4\pi} < 0.3$ , which implies the consistency limits  $M_R < 2 \cdot 10^{15}$  GeV in the hierarchical and  $M_R < 3 \cdot 10^{14}$  GeV in the degenerate case. It should be stressed in this context, that since the negative mass shift  $\delta m_L^2$  given in (27) is driven by the neutrino Yukawa couplings, the slepton masses decrease with increasing  $M_R$ . We have checked that in the perturbative region of  $Y_{\nu_3}$  defined above, the slepton masses do not violate existing lower mass bounds, in particular the LEP bound  $m_{\tilde{\tau}_1} > 81$  GeV [8].

## 5 Numerical Results

The dependence of  $Br(l_i \rightarrow l_j \gamma)$  on the right-handed Majorana mass scale  $M_R$  is displayed in Figs. 3, 4 and 5 for those two mSUGRA scenarios listed in Tab. 1 which lead to the largest and smallest branching ratios. The sensitivity on  $M_R$  for all benchmark mSUGRA scenarios defined in Tab. 1 is summarized in Tab. 3. The present bounds on  $Br(\tau \rightarrow e \gamma)$  and  $Br(\tau \rightarrow \mu \gamma)$  set relatively weak constraints on  $M_R$  and are therefore not included in Tab. 3. For each scenario, the neutrino input is varied in the ranges allowed by present and/or future experiments.

Comparing Figs. 3 and 4 with Fig. 5, one can see that  $Br(\mu \rightarrow e \gamma)$  is more strongly affected by the uncertainties in the neutrino parameters than  $Br(\tau \rightarrow \mu \gamma)$ . This finding can be understood qualitatively from (52) and (53), where one sees that  $\tau \rightarrow \mu \gamma$  mainly depends on the large angle  $\theta_{23}$  while  $\mu \rightarrow e \gamma$  involves the small quantities  $\theta_{13}$  and  $\Delta m_{12}^2$ . The difference in the scatter range of the predictions for  $\tau \rightarrow \mu \gamma$  and  $\mu \rightarrow e \gamma$  thus reflects the different relative error of the quantities  $\theta_{23}, \theta_{13}$  and  $\Delta m_{12}^2$  and also the complete lack of knowledge on  $\varphi$  (see Tab. 2). Furthermore Figs. 3, 4 and 5 and Tab. 3 show that the experimental prospects favor the channel  $\mu \rightarrow e \gamma$  over  $\tau \rightarrow \mu \gamma$  for testing small values of

Scenario	$Br(\mu \rightarrow e\gamma) = 1.2 \cdot 10^{-11}$	$Br(\mu \rightarrow e\gamma) = 10^{-14}$		$Br(\tau \rightarrow \mu\gamma) = 10^{-9}$
	$M_R/10^{14}$ GeV present/hier.	future/hier.	future/deg.	$M_R/10^{14}$ GeV future/hier.
A	[4,20]	[0.2,4]	[0.9,3]	-
B	[0.1,20]	[0.006,0.4]	[0.02,2]	[1,2]
C	[0.6,20]	[0.04,0.8]	[0.2,2]	[9,11]
D	[2,20]	[0.07,2]	[0.2,2]	[15,19]
E	[0.3,20]	[0.02,0.8]	[0.1,2]	[4,5]
F	[3,20]	[0.2,2]	[0.6,2]	-
G	[0.2,20]	[0.01,0.4]	[0.1,2]	[2,3]
H	[4,20]	[0.3,4]	[1,3]	-
I	[0.04,5]	[0.003,0.04]	[0.02,1]	[0.3,0.6]
J	[0.3,20]	[0.02,0.8]	[0.1,2]	[3,4]
K	[0.5,20]	[0.03,0.8]	[0.2,2]	[4,7]
L	[0.04,5]	[0.003,0.04]	[0.02,0.6]	[0.2,0.5]
M	[0.6,20]	[0.06,0.8]	[0.2,2]	[6,9]

Table 3: Ranges of values for  $M_R$  for the given branching ratios in the case of hierarchical or degenerate neutrino spectra with present or future uncertainties of neutrino parameters. With '-' we denote that the sensitivity is too low.

$M_R$ . Larger values of  $M_R$  would be probed more accurately in  $\tau \rightarrow \mu\gamma$ .

We also find that for fixed  $M_R$  the branching ratios for  $l_i \rightarrow l_j\gamma$  depend strongly on the particular mSUGRA scenario. The strongest bounds on  $M_R$  are obtained in scenario L due to very large  $\tan\beta$  and small sparticle masses, whereas scenario H with large gaugino masses yields the weakest bounds.

In summary, we find for hierarchical neutrino spectra that a future measurement of  $Br(\tau \rightarrow \mu\gamma) \approx 10^{-9}$  would typically determine  $M_R$  up to a factor of 2 given the uncertainties in the neutrino parameters. On the other hand, a measurement of  $Br(\mu \rightarrow e\gamma) \approx 10^{-14}$  would determine the right-handed scale only up to a factor of 10-100, even if the SUSY parameters would be known. Finally, assuming an exactly massless lightest neutrino (as in previous works), the upper bounds on  $M_R$  improve by a factor of up to 10. For degenerate neutrinos and  $M_R < 10^{14}$  GeV,  $Br(l_i \rightarrow l_j\gamma)$  is suppressed by roughly two orders of magnitude as compared to the case of hierarchical neutrino spectra, but exhibit a similar dependence on  $M_R$ .



This can be seen by comparing Figs. 3 and 4. However, for  $M_R > 10^{14}$  GeV, the neutrino Yukawa couplings increase more strongly for degenerate than for hierarchical neutrinos, as illustrated in Fig. 2. Hence for sufficiently large  $M_R$ , the branching ratios for hierarchical and degenerate neutrinos become comparable. This behaviour is particularly pronounced for  $Br(\tau \rightarrow \mu\gamma)$  as indicated in Fig. 5, because of the enhanced loop contribution from the lightest stau.

## 6 Conclusions

Future experiments searching for lepton-flavor violating rare processes can test the Majorana mass scale  $M_R$  of right-handed neutrinos in the see-saw mechanism. We have systematically and comprehensively studied the sensitivity of  $Br(l_i \rightarrow l_j\gamma)$  on  $M_R$  in mSUGRA benchmark scenarios designed for future collider studies taking into account the uncertainties of present and future neutrino measurements. We have assumed degenerate Majorana masses for the right-handed neutrinos and a normal neutrino mass hierarchy, and have considered hierarchical and degenerate neutrino spectra.

For hierarchical neutrinos the measurement of  $Br(\mu \rightarrow e\gamma) \approx 10^{-14}$  would probe  $M_R$  in the range  $5 \cdot 10^{12}$  GeV to  $5 \cdot 10^{14}$  GeV, depending on the mSUGRA scenario. On the other hand, a future measurement of  $Br(\tau \rightarrow \mu\gamma)$  at a level of  $10^{-9}$  will determine  $M_R$  in the range larger than  $5 \cdot 10^{13}$  GeV with an accuracy of a factor of 2 for a given scenario. In the case of degenerate neutrino masses the upper bound on  $M_R$  which can be derived from  $Br(\mu \rightarrow e\gamma) < 10^{-14}$  is  $(1 - 3) \cdot 10^{14}$  GeV, independently of the mSUGRA scenario. Unification of the top Yukawa coupling and the Yukawa coupling of the heaviest neutrino at  $M_X$  would fix  $M_R$  to  $M_R \approx 4 \cdot 10^{14}$  GeV and  $M_R \approx 7 \cdot 10^{13}$  GeV for hierarchical and degenerate neutrinos, respectively. This proposition can thus be tested in the future.

Planned measurements of  $\mu \rightarrow 3e$  are not expected to improve the bounds on  $M_R$ . On the other hand, a future measurement of  $R(\mu^-Ti \rightarrow e^-Ti) \approx 10^{-18}$  is found to be more sensitive to  $M_R$  by a factor of about 2 than  $Br(\mu \rightarrow e\gamma) \approx 10^{-15}$ .

The correlation between the SUSY contribution  $\delta a_\mu$  to  $g_\mu - 2$  and  $Br(l_i \rightarrow l_j\gamma)$  can be used to reduce the mSUGRA scenario dependence of the above tests. Comparing the ratio  $Br(\tau \rightarrow \mu\gamma)/(\delta a_\mu)^2$  in Fig. 6 with the branching ratio for  $\tau \rightarrow \mu\gamma$  shown in Fig. 5, one can see that for fixed  $M_R$  and different mSUGRA scenarios the ratio varies by two orders of magnitude less than the value of  $Br(\tau \rightarrow \mu\gamma)$  itself.

## Acknowledgements

We thank M. C. Gonzalez-Garcia, J. Hisano, A. Ibarra and A. Parkhomenko for useful discussions. This work was supported by the Bundesministerium für Bildung und Forschung (BMBF, Bonn, Germany) under the contract number 05HT1WWA2.

## References

- [1] Q. R. Ahmad *et al.* [SNO Collaboration], Phys. Rev. Lett. **87**, 071301 (2001) [arXiv:nucl-ex/0106015].
- [2] Y. Fukuda *et al.* [Super-Kamiokande Collaboration], Phys. Rev. Lett. **81**, 1562 (1998) [arXiv:hep-ex/9807003].
- [3] M. Gell-Mann, P. Ramond and R. Slansky, Proceedings of the Supergravity Stony Brook Workshop, New York 1979, eds. P. Van Nieuwenhuizen and D. Freedman; T. Yanagida, Proceedings of the Workshop on Unified Theories and Baryon Number in the Universe, Tsukuba, Japan 1979, eds. A. Sawada and A. Sugamoto; R. N. Mohapatra and G. Senjanovic, Phys. Rev. Lett. **44**, 912 (1980), *erratum* Phys. Rev. **D 23**, 165 (1993).
- [4] S. T. Petcov, Sov. J. Nucl. Phys. **25**, 340 (1977) [Yad. Fiz. **25**, 641 (1977 ERRAT,25,698.1977 ERRAT,25,1336.1977)]; S. M. Bilenkii, S. T. Petcov and B. Pontecorvo, Phys. Lett. B **67**, 309 (1977).
- [5] J. Hisano, T. Moroi, K. Tobe and M. Yamaguchi, Phys. Rev. D **53**, 2442 (1996) [arXiv:hep-ph/9510309].
- [6] M. L. Brooks *et al.* [MEGA Collaboration], Phys. Rev. Lett. **83**, 1521 (1999) [arXiv:hep-ex/9905013].
- [7] L. M. Barkov *et al.*, Research Proposal R-99-05.1 for an experiment at PSI (1999).
- [8] D. E. Groom *et al.* [Particle Data Group Collaboration], Eur. Phys. J. C **15**, 1 (2000) and 2001 partial update for edition 2002.
- [9] S. Ahmed *et al.* [CLEO Collaboration], Phys. Rev. D **61**, 071101 (2000) [arXiv:hep-ex/9910060].

- [10] L. Serin and R. Stroynowski, ATLAS Internal Note (1997); D. Denegri, private communication; T. Ohshima, talk at the 3rd Workshop on Neutrino Oscillations and their Origin (NOON2001), 2001, ICRR, Univ. of Tokyo, Kashiwa, Japan, to appear in the proceedings.
- [11] U. Bellgardt *et al.* [SINDRUM Collaboration], Nucl. Phys. B **299**, 1 (1988).
- [12] P. Wintz, Proceedings of the First International Symposium on Lepton and Baryon Number Violation, eds. H.V. Klapdor-Kleingrothaus and I.V. Krivosheina (Institute of Physics, Bristol, 1998), p. 534.
- [13] SINDRUM II collaboration, Research Proposal R-89-06 for an experiment at PSI (1989).
- [14] M. Bachmann *et al.* [MECO collaboration], Research Proposal E940 for an experiment at BNL (1997).
- [15] W. Ootani, talk at the 3rd Workshop on Neutrino Oscillations and their Origin (NOON2001), 2001, ICRR, Univ. of Tokyo, Kashiwa, Japan, to appear in the proceedings.
- [16] J. Aysto *et al.* [arXiv:hep-ph/0109217], Report of the Stopped Muons Working Group for the ECFA-CERN study on Neutrino Factory & Muon Storage Rings at CERN.
- [17] K. Yoshimura, talk at the 3rd Workshop on Neutrino Oscillations and their Origin (NOON2001), 2001, ICRR, Univ. of Tokyo, Kashiwa, Japan, to appear in the proceedings.
- [18] Y. Kuno and Y. Okada, Rev. Mod. Phys. **73**, 151 (2001) [arXiv:hep-ph/9909265].
- [19] J. Hisano and D. Nomura, Phys. Rev. D **59**, 116005 (1999) [arXiv:hep-ph/9810479].
- [20] J. A. Casas and A. Ibarra, Nucl. Phys. B **618**, 171 (2001) [arXiv:hep-ph/0103065].
- [21] R. Barbieri, L. Hall and A. Strumia, Nucl. Phys. B **445**, 219 (1995); G. K. Leontaris and N. D. Tracas, Phys. Lett. B **431**, 90 (1998); K. S. Babu, B. Dutta and R. N. Mohapatra, Phys. Lett. B **458**, 93 (1999) [arXiv:hep-ph/9904366]; W. Buchmuller, D. Delepine and F. Vissani, Phys. Lett. B **459**, 171 (1999); M. E. Gomez, G. K. Leontaris, S. Lola and J. D. Vergados, Phys. Rev. D **59**, 116009 (1999); S. F. King and M. Oliveira, Phys. Rev. D **60**, 035003 (1999); W. Buchmuller, D. Delepine and L. T. Handoko, Nucl. Phys. B

- 576**, 445 (2000); J. Ellis, M. E. Gomez, G. K. Leontaris, S. Lola and D. V. Nanopoulos, Eur. Phys. J. C **14**, 319 (2000); J. L. Feng, Y. Nir and Y. Shadmi, Phys. Rev. D **61**, 113005 (2000); J. Sato and K. Tobe, Phys. Rev. D **63**, 116010 (2001); D. F. Carvalho, M. E. Gomez and S. Khalil, JHEP **0107**, 001 (2001); J. R. Ellis, J. Hisano, M. Raidal and Y. Shimizu, arXiv:hep-ph/0206110.
- [22] J. Sato, K. Tobe and T. Yanagida, Phys. Lett. B **498**, 189 (2001); S. Davidson and A. Ibarra, JHEP **0109**, 013 (2001).
- [23] P. Ciafaloni, A. Romanino and A. Strumia, Nucl. Phys. B **458**, 3 (1996); J. Hisano, T. Moroi, K. Tobe and M. Yamaguchi, Phys. Lett. B **391**, 341 (1997); J. Hisano, D. Nomura, Y. Okada, Y. Shimizu and M. Tanaka, Phys. Rev. D **58**, 116010 (1998); J. Hisano, D. Nomura and T. Yanagida, Phys. Lett. B **437**, 351 (1998); S. W. Baek, N. G. Deshpande, X. G. He and P. Ko, Phys. Rev. D **64**, 055006 (2001); G. Barenboim, K. Huitu and M. Raidal, Phys. Rev. D **63**, 055006 (2001); X. J. Bi and Y. B. Dai; S. Lavignac, I. Masina and C. A. Savoy, Phys. Lett. B **520**, 269 (2001).
- [24] A. Kageyama, S. Kaneko, N. Shimoyama and M. Tanimoto, Phys. Rev. D **65** 096010 (2002) [arXiv:hep-ph/0112359].
- [25] M. Battaglia *et al.*, Eur. Phys. J. C **22**, 535 (2001) [arXiv:hep-ph/0106204].
- [26] D. F. Carvalho, J. R. Ellis, M. E. Gomez and S. Lola, Phys. Lett. B **515**, 323 (2001) [arXiv:hep-ph/0103256].
- [27] J. R. Ellis and S. Lola, Phys. Lett. B **458**, 310 (1999) [arXiv:hep-ph/9904279].
- [28] W. de Boer, Prog. Part. Nucl. Phys. **33**, 201 (1994) [arXiv:hep-ph/9402266].
- [29] J. R. Ellis, M. E. Gomez, G. K. Leontaris, S. Lola and D. V. Nanopoulos, Eur. Phys. J. C **14**, 319 (2000) [arXiv:hep-ph/9911459].
- [30] Y. Okada, K. I. Okumura and Y. Shimizu, Phys. Rev. D **61**, 094001 (2000) [arXiv:hep-ph/9906446].
- [31] J. R. Ellis, J. Hisano, S. Lola and M. Raidal, Nucl. Phys. B **621**, 208 (2002) [arXiv:hep-ph/0109125].
- [32] M. Knecht and A. Nyffeler, Phys. Rev. D **65**, 073034 (2002) [arXiv:hep-ph/0111058].

- [33] M. C. Gonzalez-Garcia, M. Maltoni, C. Pena-Garay and J. W. Valle, Phys. Rev. D **63**, 033005 (2001) [arXiv:hep-ph/0009350].
- [34] J. N. Bahcall, M. C. Gonzalez-Garcia and C. Pena-Garay, [arXiv:hep-ph/0204314].
- [35] V. Barger, D. Marfatia and B. P. Wood, Phys. Lett. B **498**, 53 (2001) [arXiv:hep-ph/0011251].
- [36] MINOS Technical Design Report,  
[http://www.hep.anl.gov/ndk/hypertext/minos\\_tdr.html](http://www.hep.anl.gov/ndk/hypertext/minos_tdr.html).
- [37] M. Apollonio *et al.* [CHOOZ Collaboration], Phys. Lett. B **466**, 415 (1999) [arXiv:hep-ex/9907037].
- [38] V. Barger, talk at Joint U.S. / Japan Workshop on New Initiatives in Muon Lepton Flavor Violation and Neutrino Oscillation with High Intense Muon and Neutrino Sources, Honolulu, Hawaii, 2000, to appear in the proceedings. [arXiv:hep-ph/0102052].
- [39] A. S. Dighe and A. Y. Smirnov, Phys. Rev. D **62**, 033007 (2000) [arXiv:hep-ph/9907423].
- [40] H. Minakata and H. Nunokawa, Phys. Lett. B **504**, 301 (2001); C. Lunardini and A. Y. Smirnov, Phys. Rev. D **63**, 073009 (2001).
- [41] V. Barger, D. Marfatia and B. P. Wood, Phys. Lett. B **532**, 19 (2002) [arXiv:hep-ph/0202158].
- [42] J. J. Gomez-Cadenas, Nucl. Phys. Proc. Suppl. **99B**, 304 (2001) [arXiv:hep-ph/0105298].
- [43] H. Päs and T. J. Weiler, Phys. Rev. D **63**, 113015 (2001) [arXiv:hep-ph/0101091].
- [44] A. Osipowicz *et al.* [KATRIN Collaboration], [arXiv:hep-ex/0109033]; C. Weinheimer, private communication.
- [45] H. V. Klapdor-Kleingrothaus, A. Dietz, H. L. Harney and I. V. Krivosheina, Mod. Phys. Lett. A **16**, 2409 (2001) [arXiv:hep-ph/0201231].

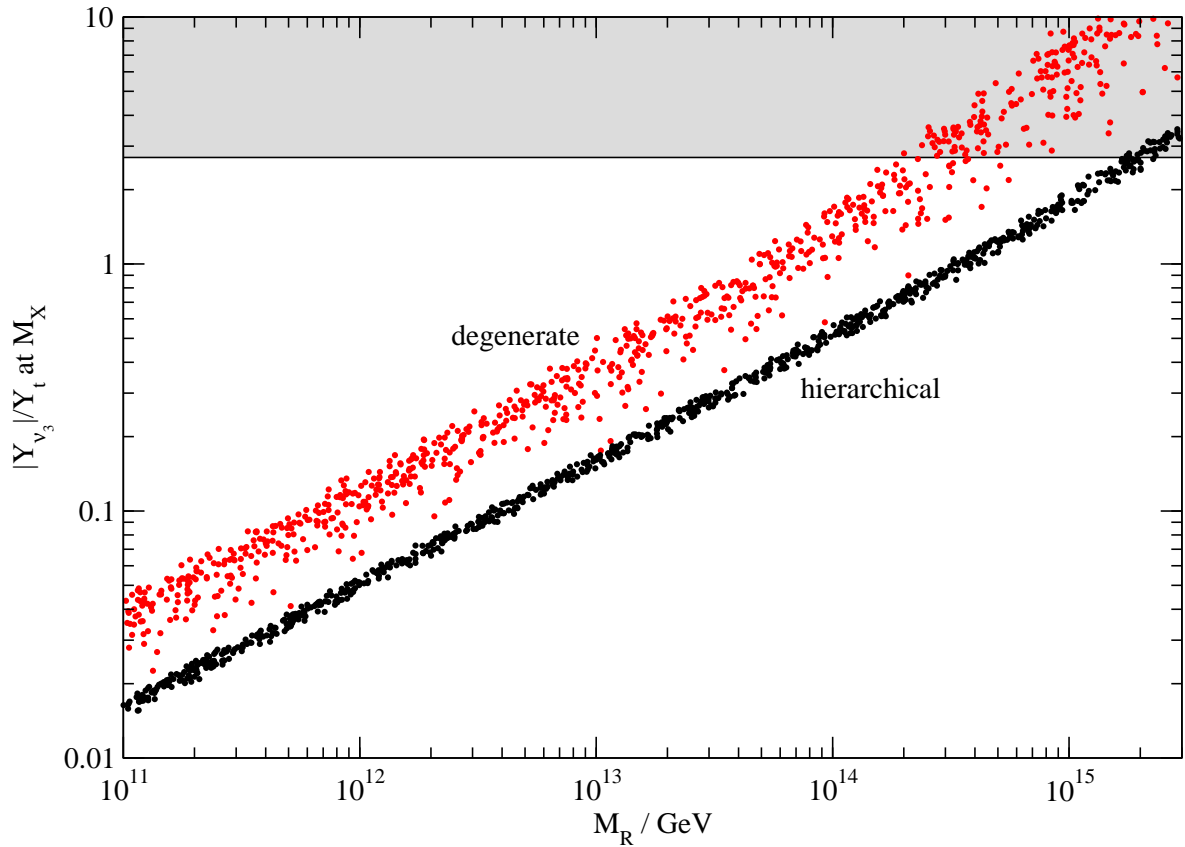


Figure 2: Largest Yukawa coupling  $|Y_{\nu_3}|$  normalized to the top Yukawa coupling  $Y_t$  at  $M_X$  for hierarchical and degenerate neutrino spectra ( $\tan \beta = 30$ ). The shaded area is excluded by the constraint  $\frac{|Y_{\nu_3}|^2}{4\pi} < 0.3$ .

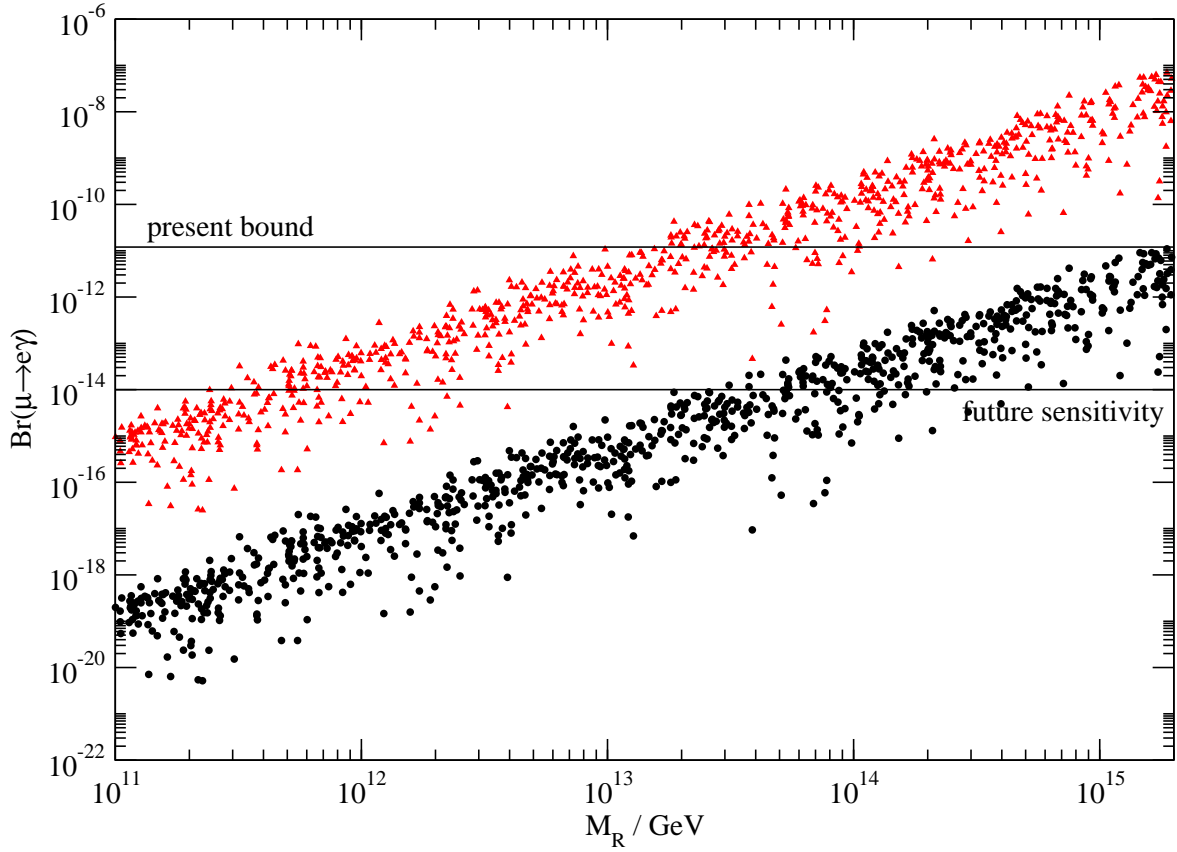


Figure 3: Branching ratio of  $\mu \rightarrow e\gamma$  for hierarchical neutrinos and uncertainties of future neutrino experiments in the mSUGRA scenarios leading to the largest (L, upper) and the smallest (H, lower) LFV rates.

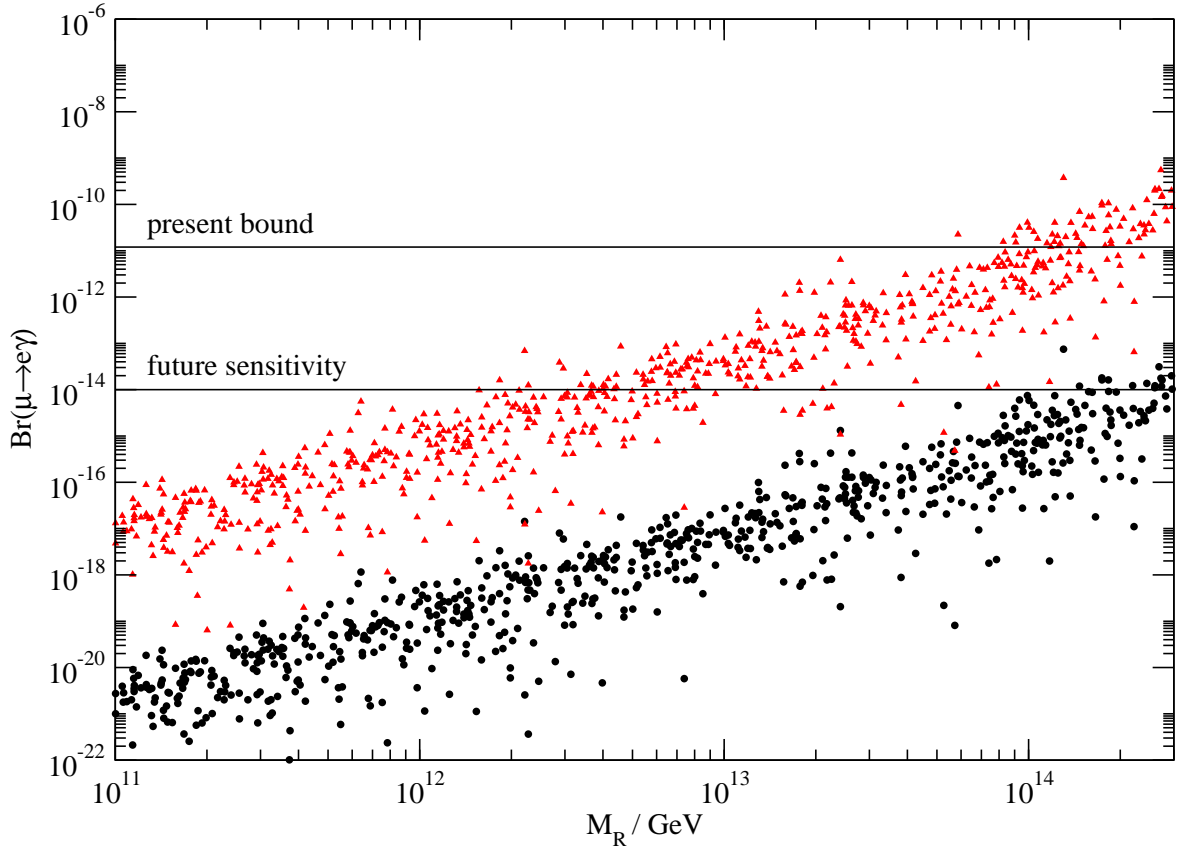


Figure 4: Branching ratio of  $\mu \rightarrow e\gamma$  for degenerate neutrinos and uncertainties of future neutrino experiments in the mSUGRA scenarios leading to the largest (L, upper) and the smallest (H, lower) LFV rates.



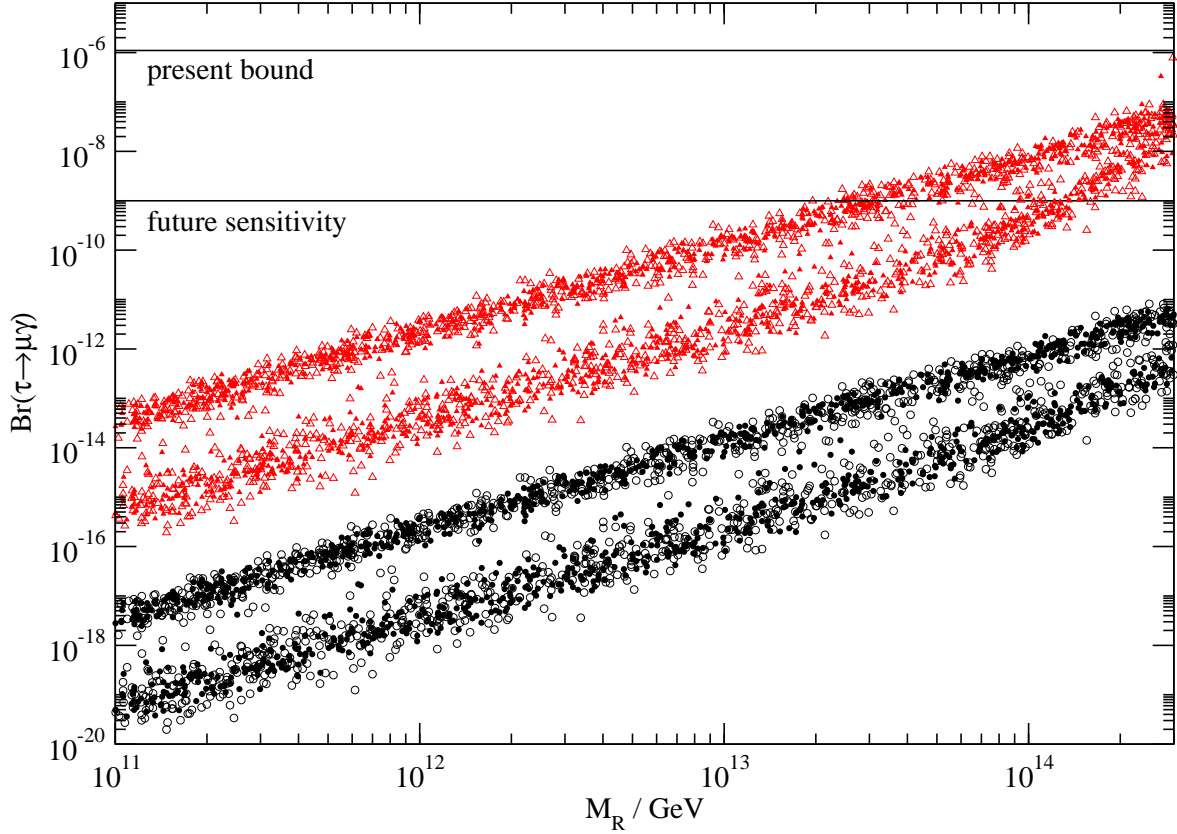


Figure 5: Branching ratio of  $\tau \rightarrow \mu\gamma$  for hierarchical (upper) and degenerate (lower) neutrino masses in the mSUGRA scenarios leading to the largest (L, triangles) and the smallest (H, circles) LFV rates. Open and filled symbols refer to neutrino measurements with present and future uncertainties, respectively.

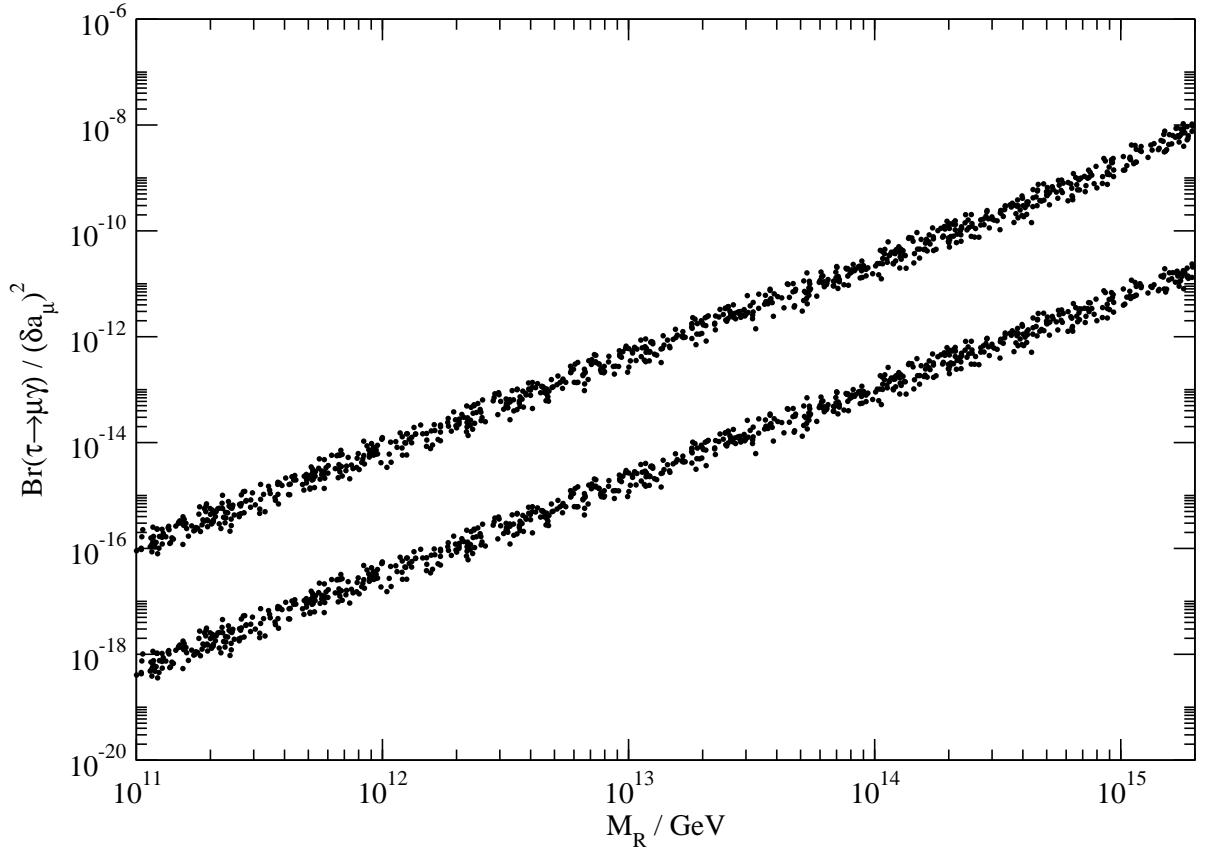


Figure 6: Ratio  $Br(\tau \rightarrow \mu\gamma)/(\delta a_\mu)^2$  for hierarchical neutrinos and uncertainties of future neutrino experiments. Shown are the expectations for the mSUGRA scenarios F (upper) and C (lower) which embrace the predictions for all other benchmark scenarios of Tab. 1.